

Anomalous oscillations in the spectra of light backscattered by inhomogeneous microparticles

Xu Li,^{1,2} Allen Taflove,² and Vadim Backman¹

¹*Department of Biomedical Engineering, Northwestern University, Evanston, Illinois 60208, USA*

²*Department of Electrical Engineering and Computer Science, Northwestern University, Evanston, Illinois 60208, USA*

(Received 10 January 2006; published 8 March 2007)

We report anomalous oscillatory features in the spectra of cross-polarized backscattered light from inhomogeneous dielectric microparticles. Numerical experiments based on the finite-difference-time-domain method demonstrate that cross-polarized backscattered spectra exhibit oscillation frequencies with two *a priori* surprising features. First, the oscillation frequencies decrease as the correlation length (L_c) of the particle's refractive index increases. Second, high-frequency oscillations exist even for L_c much smaller than the optical wavelength. These findings are exactly opposite to what is observed in co-polarized backscattering spectra, and are not expected from conventional optical scattering theory. We explain this anomalous behavior by examining the path-length distributions of the backscattered photons in the cross polarization.

DOI: [10.1103/PhysRevE.75.037601](https://doi.org/10.1103/PhysRevE.75.037601)

PACS number(s): 42.25.Dd, 61.10.Dp, 87.64.-t

Elastic light-scattering signals are widely used to noninvasively probe the structural characteristics of many natural and man-made materials. For example, the spectral, angular, and polarization parameters of light scattered from biological tissue have been demonstrated to be capable of providing clinically important diagnostic information of tissue and cellular structures on the micro/nanoscales [1–4]. In particular, in a number of applications scattering signals are recorded from an isolated single scatterer or a localized structure within a complex multiparticle system. Examples include many types of optical microscopy, flow cytometry, recently developed elastic light-scattering optical coherence tomography [5], partial-wave microscopy [6], and confocal light-scattering measurements [7]. These important applications have motivated a series of investigations for understanding single light scattering from complex particles [8–10].

The oscillation frequency of backscattering spectra is an important diagnostic parameter to optically probe the geometry of the particle. Scattering spectra from random media are critically dependent on the characteristic correlation length L_c of the refractive-index distribution [11]. However, it has not been elucidated how the backscattering spectra correlate with the internal structure of inhomogeneous particles. In this paper, we investigate this correlation for inhomogeneous particles with size on the order of a few microns, which are very relevant for optical probing of biological cells. Our numerical study based on numerical solutions of Maxwell's equations demonstrates an opposite trend in the dependency of co-polarized and cross-polarized backscattering spectra on the correlation length L_c of the particle's refractive index distribution. We explain and discuss the practical implication of the anomalous behavior in cross-polarized backscattering spectra.

Our numerical study is based on finite-difference-time-domain (FDTD) method [12], which solves the Maxwell's equations numerically for arbitrary geometries, and therefore provides accurate benchmark data for light scattering problems involving complex particle geometries. We adopt a stochastic model, the Gaussian random field (GRF) model [13], to describe the geometry of the complex internal structure of inhomogeneous particles. This model enables us to numerically generate a three-dimensional spatial distribution of re-

fractive index with predefined characteristic correlation length L_c . Following the procedures described in previous publications [9,10,14], we calculate the far-field scattered wave in the backward direction for both co-polarized ($E_{\parallel}=E_x$) and cross-polarized ($E_{\perp}=E_y$) responses of inhomogeneous dielectric spheres with a range of L_c with fixed volume-averaged refractive index $n_0=1.1$ and diameter $D=4.0\ \mu\text{m}$. The left panels of Figs. 1(a)–1(d) display the spatial maps of refractive index in x - y cross section for microparticles having GRF generated refractive-index distribution and L_c ranging from $0.2\ \mu\text{m}$ [Fig. 1(a)] to $1.2\ \mu\text{m}$ [Fig. 1(d)]. As demonstrated by these maps, smaller L_c [such as shown in Fig. 1(a)] corresponds to higher spatial frequency of the refractive-index variation. The right panels of Figs. 1(a)–1(d) show the backscattered spectra in both polarizations (E_{\parallel} and E_{\perp}) calculated with FDTD for the particle geometries displayed on the left. These spectra are plotted vs wave number $k=2\pi/\lambda$ with λ ranging from 500 nm to 1000 nm. We observe from Figs. 1(a)–1(d) that the number of oscillations in E_{\parallel} (illustrated by dotted lines) decreases as the L_c decreases. On the other hand, the cross-polarized component E_{\perp} (illustrated by solid lines) has a reversed trend in the oscillation frequency—the spectrum becomes more oscillatory with decreased L_c . The opposite trends are further demonstrated in Fig. 2, where we plot the periods of spectroscopic oscillation in k space [$\Delta k=\Delta(2\pi/\lambda)$] for both E_{\parallel} and E_{\perp} vs L_c for 17 microparticles with L_c ranging from 0.05 to $1.6\ \mu\text{m}$. Here, greater value of Δk corresponds to lower frequency in the spectroscopic oscillations. The opposite trends in the oscillatory features between the two polarizations are evident for particles with L_c greater than $0.2\ \mu\text{m}$, which is approximately half of the lower bound of wavelength range ($\lambda_{\text{min}}/2$). For particles with $L_c < \lambda_{\text{min}}/2$, the E_{\parallel} spectrum becomes more oscillatory as L_c decreases, while oscillation frequency in E_{\perp} seem to saturate (or slightly decreases) as L_c decreases.

For $L_c \geq \lambda_{\text{min}}/2$, the increase of E_{\parallel} spectra's oscillation with L_c can be explained in the context of the Born approximation, where the scattering potential in \mathbf{k} space from a weakly fluctuating dielectric volume is proportional to the Fourier transform of the spatial correlation function of

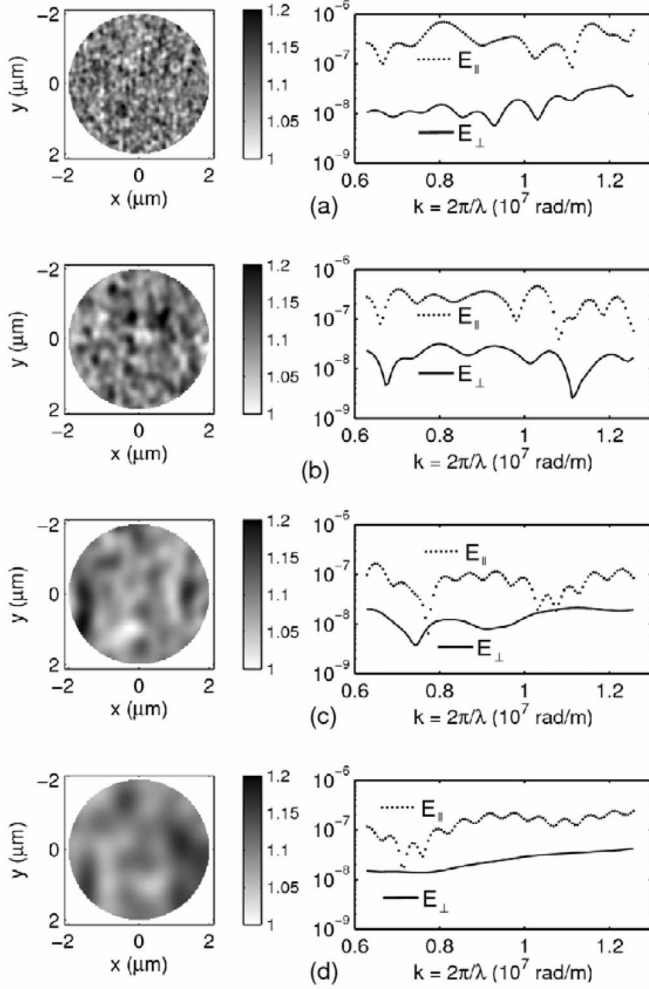


FIG. 1. FDTD calculated backscattering spectra (displayed in the right panels) of stochastically inhomogeneous microparticles (refractive-index distribution of x - y cross section displayed in the left panels). The cross-polarized component (E_{\perp}) has oscillatory features with a trend opposite to the co-polarized component (E_{\parallel}), i.e., the E_{\perp} spectra become more oscillatory as the correlation length (L_c) of the refractive-index distribution decreases. (a) $L_c = 0.2 \mu\text{m}$; (b) $L_c = 0.4 \mu\text{m}$; (c) $L_c = 0.8 \mu\text{m}$; (d) $L_c = 1.2 \mu\text{m}$.

refractive-index distribution $C_n(r) = \langle [n(0) - n_0][n(r) - n_0] \rangle$ [11]. Therefore, for refractive-index distribution with longer characteristic correlation length L_c [a wider distribution of $C_n(r)$], the scattering potential contains higher frequency components. This effect can manifest in both spectroscopic (wavelength) and angular domains. For the backscattering spectra, it presents high oscillatory frequency, as demonstrated in E_{\parallel} of Fig. 1(a). For $L_c < \lambda_{\text{min}}/2$, the scattering amplitude from each individual inhomogeneity site becomes small, and therefore the scattering spectra appear more similar to an homogeneous particle with higher oscillation frequencies. For E_{\perp} spectra of particles having $L_c \geq \lambda_{\text{min}}/2$, it is evident from Figs. 1 and 2 that the oscillation features have a dependency on L_c with an opposite trend from what is observed in co-polarized scattering spectra and what is expected based on the existing understanding of light scatter-

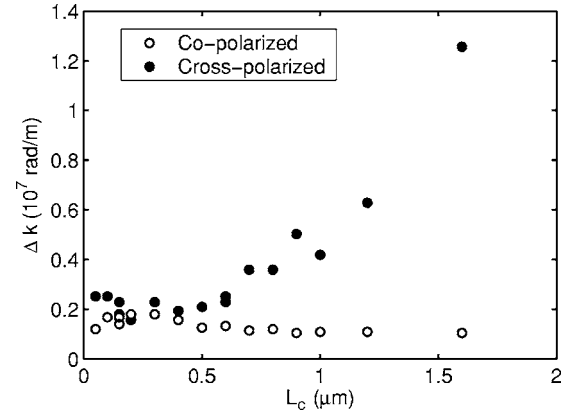


FIG. 2. Demonstration of the reversed trends in the oscillation features in co-polarized backscattering spectra and cross-polarized backscattering spectra for stochastically inhomogeneous dielectric microparticles. The periods of spectroscopic oscillation in wave-number space [$\Delta k = \Delta(2\pi/\lambda)$] of both polarizations are plotted vs L_c for 17 microparticles with L_c ranging from $0.05 \mu\text{m}$ to 1.6 . Here, Δk 's are calculated by $2(k_{\text{max}} - k_{\text{min}})/(N_{\text{max}} + N_{\text{min}})$, where k_{max} and k_{min} are upper and lower bound of the wave number range as shown in the horizontal axis of the right panel of Fig. 1, and N_{max} and N_{min} are numbers of maxima and minima in the backscattering spectra.

ing. Below we provide an interpretation of these anomalous oscillatory features.

Previously, we investigated how the overall intensity level of E_{\perp} depends on the statistical parameters of the particle's internal refractive-index distribution by examining photon path lengths and associated phase-delay distribution in different scattering planes [10]. Specifically, we considered a light ray entering the particle at position (r, φ) and exiting at $(r, \varphi + 180^\circ)$ and its counterpart in a perpendicular scattering plane. Ignoring out-of-plane scattering, the far-field cross-polarized backscattering E -field can be split into two parts with contributing photons located in orthogonal scattering planes

$$E_{\perp} = \mathcal{E}_{\perp} + \mathcal{E}_{\perp, \pi/2}, \quad (1)$$

where

$$\mathcal{E}_{\perp} = \int_0^{D/2} \left[\int_0^{\pi/2} E_{\perp}(r, \varphi) d\varphi + \int_{\pi}^{3\pi/2} E_{\perp}(r, \varphi) d\varphi \right] r dr \quad (2a)$$

and

$$\mathcal{E}_{\perp, \pi/2} = \int_0^{D/2} \left[\int_0^{\pi/2} E_{\perp}(r, \varphi + \pi/2) d\varphi + \int_{\pi}^{3\pi/2} E_{\perp}(r, \varphi + \pi/2) d\varphi \right] r dr. \quad (2b)$$

If a particle is azimuthally symmetrical (e.g., a homogeneous spherical particle), the total cross-polarized scattered field becomes zero since the contribution from photons in orthogonal planes cancelled out each other. This effect is demonstrated in Fig. 3(b), where we display FDTD-

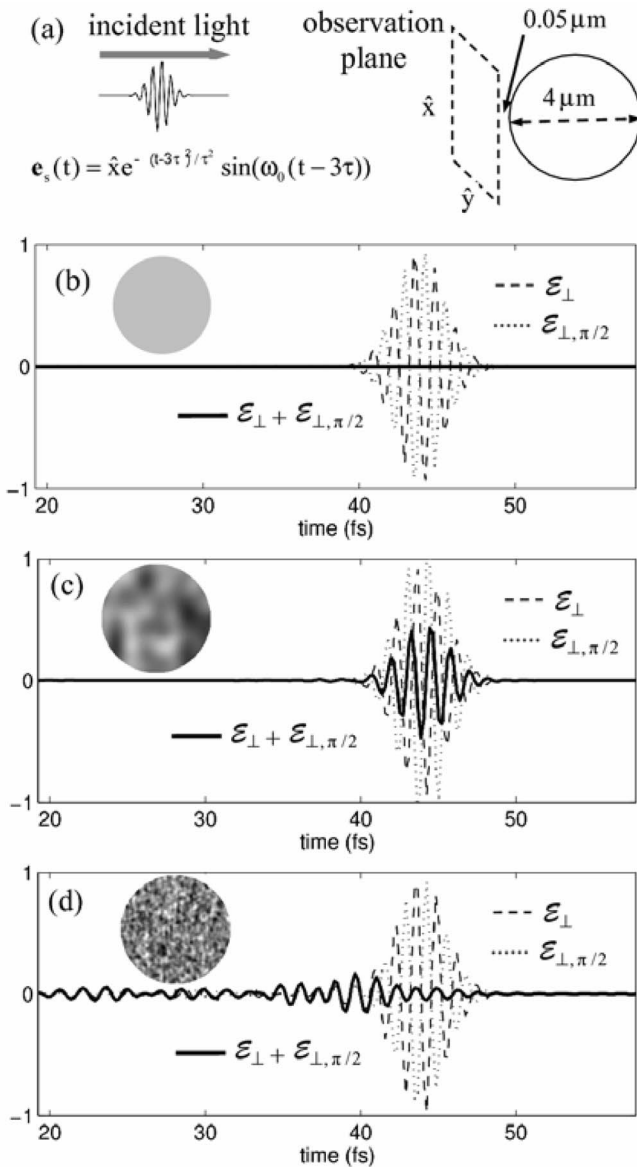


FIG. 3. FDTD-calculated time-domain waveforms of the cross-polarized components of backscattered photons. (a) Geometry of the simulation setup. A 4- μm dielectric microparticle is illuminated with \hat{x} -polarized, \hat{z} -propagating plane wave with a modulated-Gaussian time-domain waveform. (b) Cross-polarized components of backscattered E field for a homogeneous dielectric microsphere. \mathcal{E}_\perp and $\mathcal{E}_{\perp,\pi/2}$ are cross-polarized (e_y) components integrated over the observation plane and are located in scattering planes perpendicular to each other [Eq. (2)]. Due to the symmetry of the photons' path-length distribution, the combined cross-polarized component $\mathcal{E}_\perp + \mathcal{E}_{\perp,\pi/2}$ is zero. (c) For an inhomogeneous particle with $L_c = 1.2 \mu\text{m}$, \mathcal{E}_\perp and $\mathcal{E}_{\perp,\pi/2}$ do not cancel each other due to the breaking of symmetry for the path-length distribution. (d) For a particle with $L_c = 0.2 \mu\text{m}$, multiple photon paths contribute to a spreading of time-domain signal. In the frequency domain, this spreading manifests as oscillations in the spectrum.

calculated time-domain waveforms of \mathcal{E}_\perp , $\mathcal{E}_{\perp,\pi/2}$, and $\mathcal{E}_\perp + \mathcal{E}_{\perp,\pi/2}$ observed in a backscattering plane located 20 nm away from the back side of a 4- μm homogeneous sphere. For an inhomogeneous particle, photons propagating in scat-

tering planes defined by azimuth angles φ and $\varphi + \pi/2$ experience different optical path delays and are associated with different phases [$\Delta f = (2\pi/\lambda) \int \Delta n dl$] due to the variations in refractive index Δn from n_0 . As a result, the two components \mathcal{E}_\perp and $\mathcal{E}_{\perp,\pi/2}$ do not cancel each other but leave a net contribution to E_\perp . This is demonstrated in Fig. 3(c), where the cross-polarized waveforms are displayed for an inhomogeneous particle with $L_c = 1.2 \mu\text{m}$.

In the above analysis, we only considered a single path for the light ray entering the particle at position (r, φ) and exiting at $(r, \varphi + 180^\circ)$. This approximation is accurate for particles with slow spatial variation, i.e., $L_c \gg \lambda$. As L_c becomes smaller, a specific photon will be scattered by local inhomogeneities and travel multiple paths both within and outside of the scattering plane associated with optical path-length ℓ_m 's. For homogeneous particles, the distribution of pathlength $P(\ell_m)$ is a narrow distribution peaked around $\ell_0 = 2n_0D$, where n_0 is the refractive index and D is the particle diameter. For inhomogeneous particles, $P(\ell_m)$ has both a shifted peak due to variations in refractive index (as discussed in the previous paragraph) and a broadened distribution due to the multiple scattering paths. The contributions from these multiple paths interfere with each other. Since the contribution from longer paths ($\ell_m > \ell_0$) is usually associated with low scattering amplitudes, the range of path lengths contributing to the total scattering field can be estimated by $\Delta\ell = \ell_0 - \ell_{\min}$, where ℓ_{\min} is the minimum optical pathlength and is on the order of $2n_0L_c$. Therefore, a smaller L_c results in a broader distribution of $P(\ell_m)$ and higher oscillation frequency of in the backscattering spectrum. For $L_c \rightarrow 0$, $\Delta\ell$ is on the order of $\ell_0 = 2n_0D$, which results in an oscillation in backscattering spectra due to interference. The period of this oscillation in the wave-number space is estimated as follows:

$$\Delta k \sim 2\pi/n_0D. \quad (3)$$

For a 4- μm particle with average refractive index $n_0 = 1.1$, Δk is estimated as 1.4×10^6 rad/m, which agrees with the data presented in Fig. 2 for $L_c = 0.2 \mu\text{m}$. The spreading of $P(\ell_m)$ for particles with small L_c is demonstrated in Fig. 3(d), where we display the cross-polarized waveforms for an inhomogeneous particle with $L_c = 0.2 \mu\text{m}$. Here, we see early returns of E_\perp components due to the shorter path length introduced by scattering by local inhomogeneities. The spreading of responses in the time domain corresponds to the high-frequency oscillatory features in the spectral domain [Fig. 1(d)]. As L_c further decreases ($L_c < \lambda_{\min}/2$), there is a slight decrease in the oscillation frequency due to the reduced scattering amplitude from each inhomogeneity site. However, high-frequency oscillations exist even for L_c much smaller than the optical wavelength, which is not expected from conventional optical scattering theory.

In summary, in this paper, we report on anomalous oscillatory features in the spectra of cross-polarized backscattered light from inhomogeneous dielectric microparticles. Numerical solutions of Maxwell's equations using the finite-difference-time-domain method show that the oscillation frequencies of both the co-polarized and cross-polarized

backscattered spectra are critically dependent on L_c of the refractive-index distribution of the microparticle. Specifically, we demonstrate that cross-polarized backscattered spectra exhibit oscillation frequencies with two *a priori* surprising features. First, the oscillation frequencies decrease as L_c increases. Furthermore, high-frequency oscillations exist even for L_c much smaller than the optical wavelength. These findings are exactly opposite to what is conventionally expected from optical scattering theory. We explain this anomalous behavior by examining the path-length distributions of the backscattered photons in the cross polarization. By pro-

viding insights on how the oscillatory features in the back-scattering spectra depend on the particle's structural characteristics, the observations and analysis presented in this paper may facilitate the use of light-scattering based techniques to characterize micro-nano structures in biological tissues and cells.

This study was supported by NSF Grant Nos. BES-0238903, NIH R01CA11231, and NIH R01EB003682. The computational resource was provided in part by the NSF Teragrid under Project No. TG-MCB 040062N.

-
- [1] V. Backman, M. B. Wallace, L. T. Perelman *et al.*, Nature (London) **406**, 35 (2000).
- [2] L. T. Perelman, V. Backman, M. Wallace *et al.*, Phys. Rev. Lett. **80**, 627 (1998).
- [3] J. W. Pyhtila, R. N. Graf, and A. Wax, Opt. Express **11**, 3473 (2003).
- [4] H. K. Roy, Y. Liu, R. K. Wali *et al.*, Gastroenterology **126**, 1071 (2004).
- [5] D. C. Adler, T. H. Ko, P. R. Herz *et al.*, Opt. Express **12**, 5487 (2004).
- [6] Y. Liu, X. Li, Y. L. Kim *et al.*, Opt. Lett. **30**, 2445 (2005).
- [7] H. Fang, L. Qiu, S. Salahuddin *et al.*, in *Biomedical Optics Topical Meeting*, FL, USA, (2006).
- [8] Z. Chen, A. Taflove, and V. Backman, Opt. Lett. **28**, 765 (2003).
- [9] X. Li, Z. G. Chen, A. Taflove *et al.*, Phys. Rev. E **70**, 056610 (2004).
- [10] X. Li, A. Taflove, and V. Backman, Opt. Lett. **30**, 902 (2005).
- [11] A. Ishimaru, *Wave Propagation and Scattering in Random Media* (Academic Press, New York, 1978).
- [12] A. Taflove and S. Hagness, *Computational Electrodynamics: The Finite-Difference Time-Domain Method* (Artech, Boston, 2005).
- [13] R. J. Adler, *The Geometry of Random Fields* (Wiley, New York, 1981).
- [14] X. Li, A. Taflove, and V. Backman, IEEE Antennas Wireless Propag. Lett. **4**, 35 (2005).